

Rietveld Analysis on X-Ray Diffraction of South Kalimantan Kaolin Clays

Ruliana Febrianti¹, Firda Herlina², Muhammad Saukani²,

¹Department of Civil Engineering, Faculty of Engineering
Universitas Islam Kalimantan MAB, Indonesia

²Department of Mechanical Engineering, Faculty of Engineering
Universitas Islam Kalimantan MAB, Indonesia
saukani@uniska-bjm.ac.id

DOI: [10.20527/bipf.v6i2.4922](https://doi.org/10.20527/bipf.v6i2.4922)

ABSTRACT: At least 13 million tons of kaolin claystone lie in several regencies of South Kalimantan covering Banjar, Tapin, Hulu Sungai Utara and Kotabaru regencies. This paper reports an attempt to explore their crystalline state characteristics, projecting their potential use for geopolymer. Sungai Tabuk, Cintapuri and Tatakan, due to their largest kaolin claystone deposits, were chosen as the sampling sites. The kaolin samples were prepared by syphoning method prior to X-ray diffraction (XRD) characterizations in determining their crystalline phases. X'Pert HighScore Plus and Rietica software were respectively responsible for the qualitative and quantitative phase analyses. The qualitative analysis used search and match method at peak position and peak height between measured and calculated diffraction patterns. Our study revealed the existence of two main phases in the sample, i.e. quartz (SiO_2) and kaolinite ($\text{Al}_2\text{Si}_2\text{O}_5(\text{OH})_4$). In addition, the Quantitative analysis used the Rietveld method with the least squares method approach. Rietveld refinement was based on a goodness of fit score of less than 4% by minimizing the difference in the character of the diffraction pattern (position, height, width and peak shape) between the observed and the calculated XRD patterns. The Rietveld quantitative analysis shows, Tatakan is an area with kaolinite-richest deposit ($\pm 84\%$), followed by Cintapuri ($\pm 76\%$) and Tabuk ($\pm 70\%$); quartz is found in reverse.

Keywords: Kaolin, Rietveld, XRD.

INTRODUCTION

Kaolin, one of the most naturally abundant clay minerals, has been applied in many industries for years. The white-colored pure kaolin contains 84% of ($\text{Al}_2\text{Si}_2\text{O}_5(\text{OH})_4$) and 16% of ($\text{K}_{0.8}\text{Al}_2(\text{Si}_{3.2}\text{Al}_{0.8})\text{O}_{10}(\text{OH})_2$). The mined kaolin's containing phase depends on the origin and the environmental deposition. Kaolin mainly used for porcelain, paints, pharmaceuticals, cosmetics, textiles, rubber, water

treatment, the paper, and as the absorbent in medicines (Mohsen & Mostafa, 2010; Roy, Kar, Bagchi, & Das, 2015). To date, kaolin-based geopolymer is meant to replace conventional cement (Tippayasam et al., 2014) due to its thermoplastic stability against coking coal (Meng et al., 2017).

Geopolymer firstly introduced by Davidovits in the 1980s which is anorganic aluminosilicate formed by poly(sialates) family including

poly(sialate), poly(sialate-siloxo) and poly(sialate-disiloxo) (Davidovits, 1991). Kaolin is the main mineral formed by siloxo-sialates. Kaolin calcined so dehydroxylation happens to form metakaolin and then applied as geopolymer material. Geopolymer applying based on atomic ratio Si:Al. Si:Al = 1,0 can be applied to bricks, ceramics, and heat resistant floors manufacturing, while atomic ratio Si:Al = 2,0 is used in concrete and low CO₂ cement manufacturing, and for high technology application it applied to radioactive and poison encapsulation. While atomic ratio Si:Al = 3,0 can be used as metal molding and fiber matrix composite for manufacturing fire resistant material (Okoye, Durgaprasad, & Singh, 2015).

Mineral and chemical compositions of the kaolin are strongly dependent on the climate and the shape of the mineral, and processes of cleaning impurities (Baoumy, 2012). It leads to the variety of mineral contents in different regions. In addition, characterization of kaolin is very crucial to further investigate its potential application, especially in geopolymer material application. Studies on exploring the kaolin in South Kalimantan, however, has not been reported yet. This work, therefore, shows the XRD pattern of kaolin clay

which purification with syphoning and the quantitative analysis by Rietveld refinement method to determine crystalline phase composition in South Kalimantan's kaolin.

LITERATURE REVIEWS

Kaolin

Clay is a type of soil derived from natural rocks, especially feldspar rocks containing alumina silicate hydrate. These materials are generally very fine with particle sizes less than 2 microns. (Murray, 2006). One type of clay is kaolin. Kaolin has a hydrated alumina silicate (Al₂Si₂O₅(OH)₄) composition, accompanied by several accompanying minerals. Kaolin has a two-stage structure of phyllosilicates with a ratio of tetrahedral silica (Si₂O₅)²⁻ : Octahedral alumina Al₂(OH)₄²⁺ (1:1).

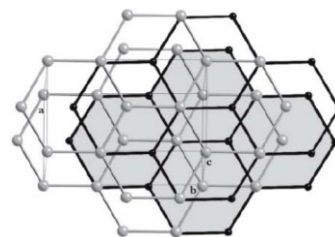


Figure 1 Structure of kaolinite, Si⁴⁺ ions (light) and Al³⁺ ions (dark) (Karmous, 2011)

In South Kalimantan itself, 13,116,000 tons of kaolin have been identified. It can be found in Hulu Sungai Utara, Tapin, Banjar and Kotabaru regencies (Saukani & Febrianty, 2017). It brings various

impurities as a natural mineral, for instance, quartz, feldspar, rutile, anatase, pyrite, and siderite (Brigatti, Galan, & Theng, 2006).

Rietveld Refinement

The refinement was evaluated by changing the related diffraction parameters following Eq. 1:

$$y_{ci} = s \sum_K L_K |F_K|^2 \phi(2\theta_i - 2\theta_K) P_K A + y_{bi} \quad (1)$$

where *i* is the index for a point being calculated, *s* is a scale factor, *K* denotes the Miller index *h, k, l* for a Bragg peak, *L_K* contains Lorentz polarization and folding factors, $|F_K|$ is the structural factor for Bragg reflection to *K*, ϕ is the peak shape function, $2\theta_i$ and $2\theta_K$ are the angles of the detector corresponding to point *i* and the peak of Bragg *K*, *P_K* is the preferred orientation function, *A* is

the absorption factor and *y_{bi}* is the background contribution.

The Rietveld refinement is based on the difference minimalization between the observed and the calculated XRD patterns, as given in Eq. 2.

$$s = \sum_K w_i (y_i - y_{ci})^2 \quad (2)$$

where *y_i* is the measured intensity at data point *i*-th, *y_{ci}* is calculated the value, and *w_i* the weighting factor for point *i*. The refinable parameters are depicted in Table 1, i.e. Bragg angle, peak intensity, peak width and peak shape (Pratapa & O'Connor, 2009) in which are available in Rietica, based on least squares approach. The accepted goodness of fit (GoF) must be less than 4%.

Table 1 Relation diffraction peak behavior with intensity diffraction model parameters

| Character | Crystal parameter | • Parameter of instrument |
|-------------------------|---|---|
| Position of peak | <ul style="list-style-type: none"> • Lattice parameter • Asymmetry | <ul style="list-style-type: none"> • 2θ error • Shift of specimen |
| Height of peak | <ul style="list-style-type: none"> • Scala factor • Asymmetry • thermal parameter • Preferred-orientation • Extinction | - |
| Width and shape of peak | <ul style="list-style-type: none"> • U, V, W, HL • Asymmetry | - |

MATERIALS AND METHODS

Kaolin samples are collected from Tatakan (TT), Cintapuri (CT) and Sungai Tabuk (ST) sub-district which

covered in Dahor Formation. Laboratory grade NaOH and H₂O₂ reagent were obtained from Aldrich. Samples are prepared by syphoning method,

following the step provided by Saukani & Febrianty to get high qualities of kaolin (Saukani & Febrianty, 2017).

The elemental composition analysis is carried out by X-Ray fluorescence (XRF) using ARL QUANT'X EDXRF. Crystallization behaviour is examined by means of X-ray diffraction using Philips X'Pert Pro, operating at 35 mA, 40 kV with a step size of 0.02 from 10° to 90° and Cu K α wavelength of 1,54060 Å. The qualitative analysis was conducted by the search-match method with X'Pert High Score Plus software. The quantitative analysis was run by Rietveld refinement method through Rietica software.

RESULTS AND DISCUSSION

The XRD profiles of the kaolin samples are shown in 2. The phase identification analysis revealed the presence of kaolinite (Al₂Si₂O₅(OH)₄, JCPDS 29-1488) and quartz (SiO₂, JCPDS 45-0131) (Saukani & Febrianty, 2017), supported by the XRF data as shown in Table 2. This data shows that TT is the most potential sample to be applied as a raw material of

geopolymer. Though the XRF data indicates the existence of some faintly minor phases, only kaolinite and quartz be found in the sample. The absence of any phases containing Fe, Ti, and K oxides is due to the very low peak intensities with which correspond to those phases.

Our result is similar to kaolin deposit found in Sarawak, Malaysia. In contrast, unwanted phases like bayerite, illite, muscovite and smectite are discovered respectively in Ipoh, Mersing, and Bidor; Malaysia (Baioumy, 2012). Muscovite and alunite are also originated in Ranong Province, Thailand (Tippayasam et al., 2014).

Rietveld analysis of samples is used to determine phase composition that contains in each sample. Crystallography parameters used as a calculated model is space group, lattice parameter, and atomic position. Crystallography data for kaolinite phase using Brindley (1977) and quartz phase using Young et al., (1977), while parameter instrument using Pratapa & O'Connor (2009). All parameters gradually refined by Rietica Software.

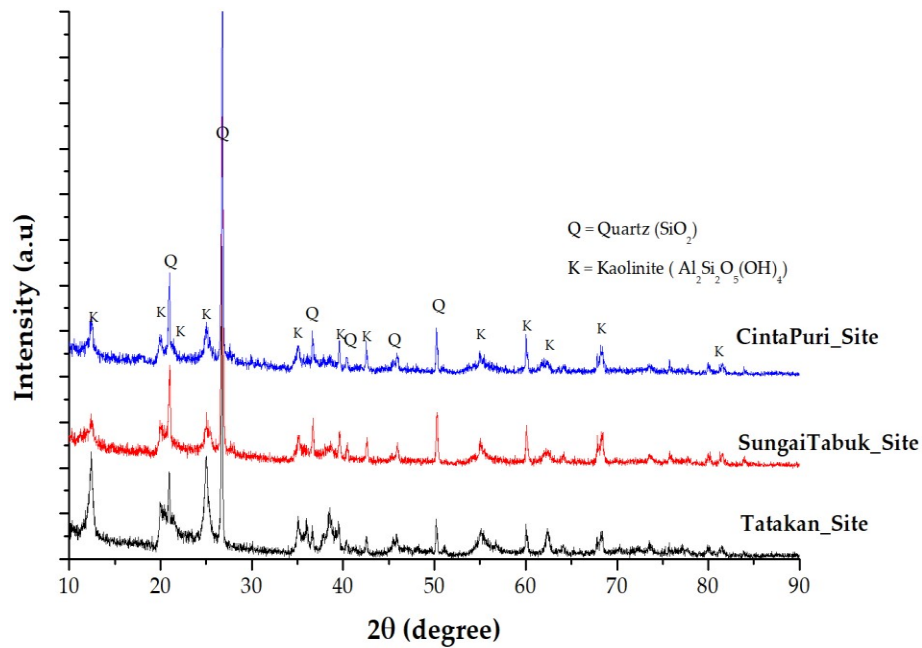


Figure 2 XRD profiles of South Kalimantan Kaolin (Saukani & Febrianty, 2017)

Table 2 Chemical composition of kaolin from CT, ST and TT

| Sample | SiO ₂ (wt%) | Al ₂ O ₃ (wt%) | Fe ₂ O ₃ (wt%) | K ₂ O (wt%) | TiO ₂ (wt%) | OCC (wt%) |
|--------|---------------------------|---|---|---------------------------|---------------------------|--------------|
| CT | 72.54 | 11.84 | 8.47 | 2.75 | 2.02 | 2.38 |
| ST | 75.37 | 13.48 | 6.78 | 2.33 | 1.77 | 0.27 |
| TT | 72.98 | 21.08 | 2.33 | 1.08 | 2.60 | 0.13 |

The Rietveld refinement plots for CT, ST, and TT XRD patterns are captured in Fig. 3, Fig. 4, and Fig. 5,

respectively. The refinement is accepted after the figure of merit establishment, see Table 2.

Table 3 Figure of merit of the Rietveld refinement of the as-prepared kaolin

| Samples | Figure-of-Merit | | |
|---------|-----------------|--------|------|
| | Rp(%) | Rwp(%) | GoF |
| CT | 18.96 | 24.83 | 1.90 |
| ST | 18.51 | 24.14 | 1.88 |
| TT | 19.24 | 25.10 | 2.16 |

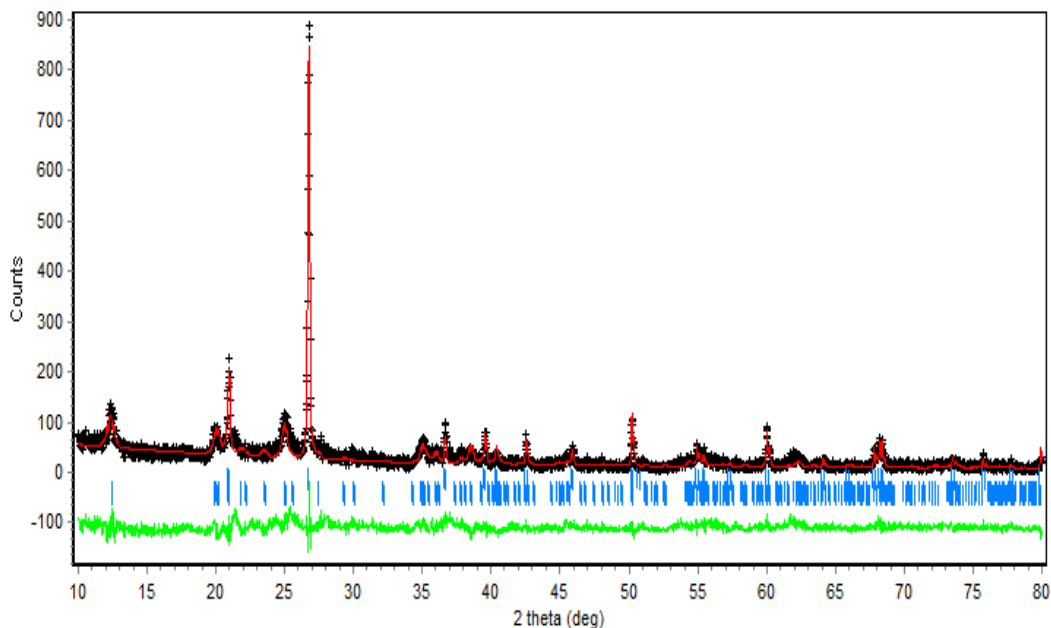


Figure 3 Rietveld refinement fitting for CT kaolin. The observed data are given by a plus sign and the calculated data by a solid red line. Vertical upper and lower blue lines indicate respectively the peak positions of quartz and kaolinite. The green line under the plot is the difference profile.

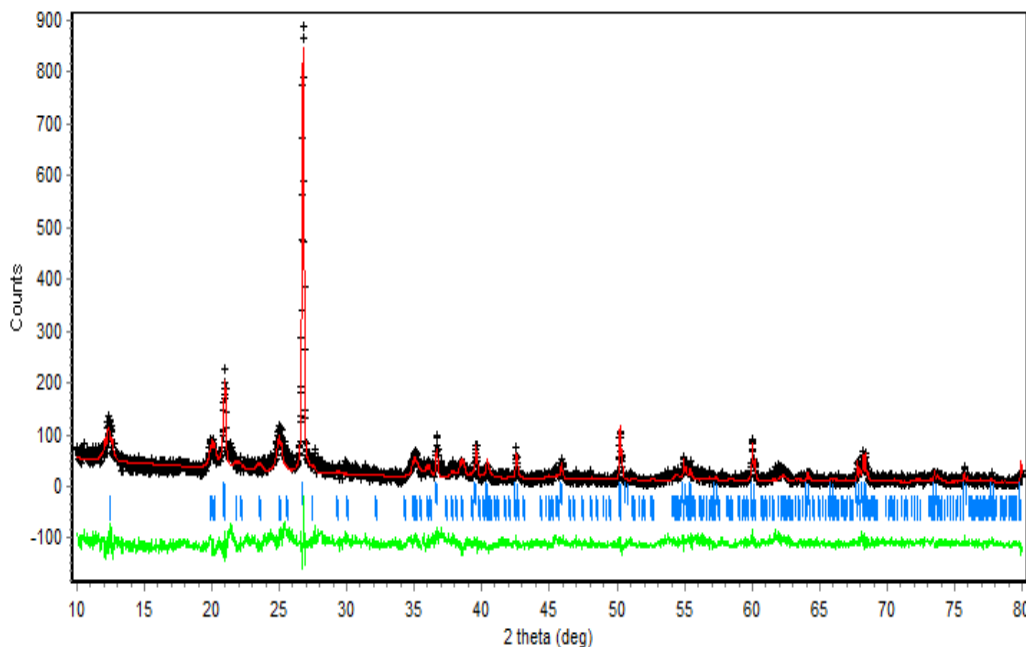


Figure 4 Rietveld refinement fitting for CT kaolin. The observed data are given by a plus sign and the calculated data by a solid red line. Vertical upper and lower blue lines indicate respectively the peak positions of quartz and kaolinite. The green line under the plot is the difference profile.

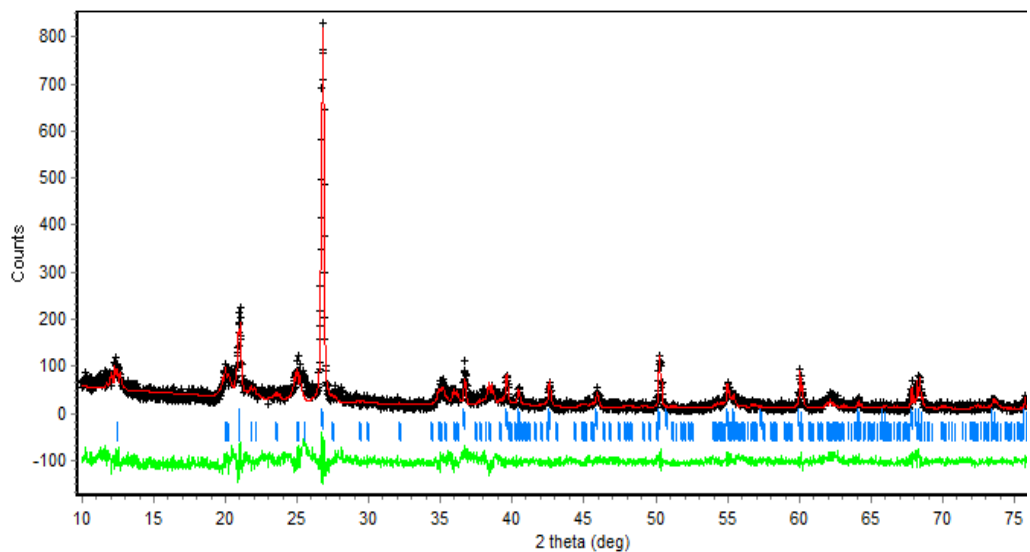


Figure 5 Rietveld refinement fitting for CT kaolin. The observed data are given by a plus sign and the calculated data by a solid red line. Vertical upper and lower blue lines indicate respectively the peak positions of quartz and kaolinite. The green line under the plot is the difference profile.

Lattice parameters and calculated crystal density can be known from Rietveld analysis, other than phase quantification. In this research, the phase weight fraction for Quartz and kaolinite phase contained in the respective samples were for ST $30.42 \pm 0.98\%$, $69.58 \pm 3.17\%$, CT $23.78 \pm 1.06\%$, $76.22 \pm 4.96\%$ and TT $84.23 \pm 3.21\%$, $15.77 \pm 1.74\%$. Clearly, Tatakan is an area with kaolinite-richest deposit, followed by Cintapuri and Sungai Tabuk. It does make sense since the degree of weathering, controlled by composition and nature of pre-existing rocks, tectonic setting, fracturation, prevailing climate conditions, vegetation, topography, CO_2 level, and biological activities plays a vital role in determining the content of crystalline

phases within the naturally occurring materials (Baioumy, 2012).

CONCLUSIONS

To conclude, all the three different sites provide the huge amount of kaolinite, which is above 70%. In terms of XRD profiles of Tatakan, Cintapuri, and Sungai Tabuk, the sequences of 2θ -intensity of either kaolinite or quartz show excellent similarities. Tatakan, in addition, is the best region for exploring kaolinite deposit and the most potential sample to be applied as a raw material of geopolymer.

ACKNOWLEDGMENTS

The authors acknowledge the support of the following for this project financial

support for Universitas Islam Kalimantan MAB through APBU UNISKA 2017.

REFERENCES

- Baioumy, H. (2012). Mineralogical Variations among the Kaolin Deposits in Malaysia. https://doi.org/10.5176/2251-3361_GEOS12.77
- Brigatti, M. F., Galan, E., & Theng, B. K. G. (2006). Chapter 2 Structures and Mineralogy of Clay Minerals. In F. Bergaya, B. K. G. Theng, & G. Lagaly (Eds.), *Developments in Clay Science* (Vol. 1, pp. 19–86). Elsevier. [https://doi.org/10.1016/S1572-4352\(05\)01002-0](https://doi.org/10.1016/S1572-4352(05)01002-0)
- Brindley, G. (1977). *ICDD Grant-in-Aid*. PA 16801, USA: Pennsylvania State University, University Park.
- Davidovits, J. (1991). Geopolymers. *Journal of Thermal Analysis*, 37(8), 1633–1656. <https://doi.org/10.1007/BF01912193>
- Karmous, M. S. (2011). Theoretical Study of Kaolinite Structure; Energy Minimization and Crystal Properties. *World Journal of Nano Science and Engineering*, 01(02), 62. <https://doi.org/10.4236/wjnse.2011.12009>
- Meng, F., Gupta, S., Yu, J., Jiang, Y., Koshy, P., Sorrell, C., & Shen, Y. (2017). Effects of kaolinite addition on the thermoplastic behaviour of coking coal during low temperature pyrolysis. *Fuel Processing Technology*, 167, 502–510. <https://doi.org/10.1016/j.fuproc.2017.08.005>
- Mohsen, Q., & Mostafa, N. Y. (2010). Investigating the possibility of utilizing low kaolinitic clays in production of geopolymer bricks. *Ceramics Silikat*, 54(2), 160–168.
- Okoye, F. N., Durgaprasad, J., & Singh, N. B. (2015). Mechanical properties of alkali activated flyash/Kaolin based geopolymer concrete. *Construction and Building Materials*, 98, 685–691. <https://doi.org/10.1016/j.conbuildmat.2015.08.009>
- Pratapa, S., & O'Connor, B. (2009). Development of MgO Ceramic Standards for X-ray and Neutron Line Broadening Assessments. *Advanced X-Ray Analysis*, 16, 1–7.
- Roy, S., Kar, S., Bagchi, B., & Das, S. (2015). Development of transition metal oxide–kaolin composite pigments for potential application in paint systems. *Applied Clay Science*, 107, 205–212. <https://doi.org/10.1016/j.clay.2015.01.029>
- Saukani, M., & Febrianty, R. (2017). Analisa Komposisi Fasa Lempung Kalimantan Selatan Berdasarkan Data Difraksi Sinar X. *Jurnal Fisika FLUX*, 13(2), 117–120.
- Tippayasam, C., Keawpapasson, P., Thavorniti, P., Panyathanmaporn, T., Leonelli, C., & Chaysuwan, D. (2014). Effect of Thai Kaolin on properties of agricultural ash blended geopolymers. *Construction and Building Materials*, 53, 455–459. <https://doi.org/10.1016/j.conbuildmat.2013.11.079>

Young, R. A., Mackie, P. E., & von Dreele, R. B. (1977). Application of the pattern-fitting structure-refinement method of X-ray powder diffractometer patterns.

Journal of Applied Crystallography, 10(4), 262–269.
<https://doi.org/10.1107/S0021889877013466>